

# Estimating Specific Absorption Rate (SAR) during MRI in the human brain with intracranial EEG electrodes used for epilepsy monitoring: A preliminary study using finite integral technique (FIT) modelling.

D. W. Carmichael<sup>1</sup>, Y. Li<sup>2</sup>, A. McEvoy<sup>3</sup>, J. W. Hand<sup>2,4</sup>, and L. Lemieux<sup>1</sup>

<sup>1</sup>Department of Clinical and Experimental Epilepsy, UCL Institute of Neurology, London, United Kingdom, <sup>2</sup>Imaging Sciences Department, MRC Clinical Sciences Centre, Imperial College, London, United Kingdom, <sup>3</sup>Victor Horsley Department of Neurosurgery, National Hospital for Neurology and Neurosurgery, London, United Kingdom, <sup>4</sup>Radiological Sciences Unit, Imperial College Healthcare NHS Trust, London, United Kingdom

**Introduction** MRI is advantageous for localising intracranial EEG electrodes used for epilepsy monitoring due to good visualisation of implant position relative to the neuroanatomy and the avoidance of the radiation dose associated with CT. However, RF-induced increased heating around such implants poses a potential health hazard<sup>1</sup>.

**Methods** Simulations were performed using a commercial software package, the Transient Solver was used to solve the electromagnetic problem within CST Microwave Studio® v2006B (Computer Simulation Technology, Darmstadt, Germany). This provides a solution to the time-dependent Maxwell's equations using a time-domain variant of the finite integration technique<sup>2,3</sup> (FIT). FIT uses the integral forms of Maxwell's equations, and transforms them into a set of matrix equations to obtain  $E$  ( $V m^{-1}$ ), the electric field strength, and  $B$  ( $T$ ) the magnetic flux density,  $H$  ( $A m^{-1}$ ). Specific absorption rate (SAR) was then calculated using the software's IEEE C95.3 averaging method over both 1g and 10g of tissue from the power loss density at 62.5MHz with 1W peak input power. The model consisted of three main parts: 1) a generic design 16 rung birdcage head transmit RF-coil with internal diameter of 280 mm and length 300mm. The end rings were 10 mm wide, 90.5pF capacitors were inserted in 5mm gaps equi-distant from each rung; this tuned the coil to have a principal resonance at the approximate frequency of a 1.5T scanner (62.5MHz). In two of these gaps at 135° and 225° relative to the vertical (y) axis the coil was driven by application of a voltage in quadrature; 2) a head-torso model was used of resolution 1.66x1.66x2mm derived from imaging a 23 year-old male and segmenting the images into 32 different tissue types<sup>4</sup>. Each tissue was assigned density, permittivity, and conductive properties (calculated using <http://www.fcc.gov/fcc-bin/dielec.sh> and <http://niremf.ifac.cnr.it/tissprop/htmlclie/htmlclie.htm>)<sup>4</sup>; 3) an implant approximating an Ad-tech (Racine, WI, USA) electrode grid (a 6x8 array of 3mm diameter Pt-Ir disk contacts with 10mm spacing within a silicon sheet, and tails (1 per row of contacts) comprising of 0.1mm stainless steel (316) wires and Ni-Cr tail contacts contained within polyurethane tubing, total length 455mm). The implant was positioned to lie at the brain surface over the left temporal/parietal area. The model was run both with and without the implant.

**Results** The electric field was found to be focussed around the implant, in particular around the distal (most inferior relative to the brain) contacts (see fig. 1a). A comparison was made between the peak E-field in two different planes: 1) the sagittal plane adjacent to the grid electrode ( $x=-68$ mm, all values relative to the origin in the coil centre); 2) the axial plane bisecting the distal grid contacts ( $z=8$ mm) both with and without the implant (table 1). The maximum E-field value within the head was much greater with the implant than without, and was adjacent to the grid's most anterior distal contact (table 1). The peak SAR values and positions (within the same planes 1 & 2) were dependent on the averaging mass. For the 1g average the maximum was by the most anterior distal contact but not for the 10g average (table 2). For both 1g and 10g averages the maximum local SAR lay in the sinus region (as for the head-only model) away from the implant.

Slice position	Mass average	SAR (W/Kg)	Position
1) sagittal $x=-68$	1g	0.49	anterior-/inferior-most contact
2) axial $z=8$		0.61	sinus
1) sagittal $x=-68$	10g	0.28	20mm inferior to grid
2) axial $z=8$		0.38	sinus

Table 2 SAR maxima in the head with the implant present

Slice position	Implant present	E-field (V/m)	Position
1) sagittal $x=-68$	No	107	sinus
2) axial $z=8$		498	sinus
1) sagittal $x=-68$	Yes	984	anterior-/inferior-most contact
2) axial $z=8$		1883	anterior-/inferior-most contact

Table 1 Comparison of E-field maxima within the head

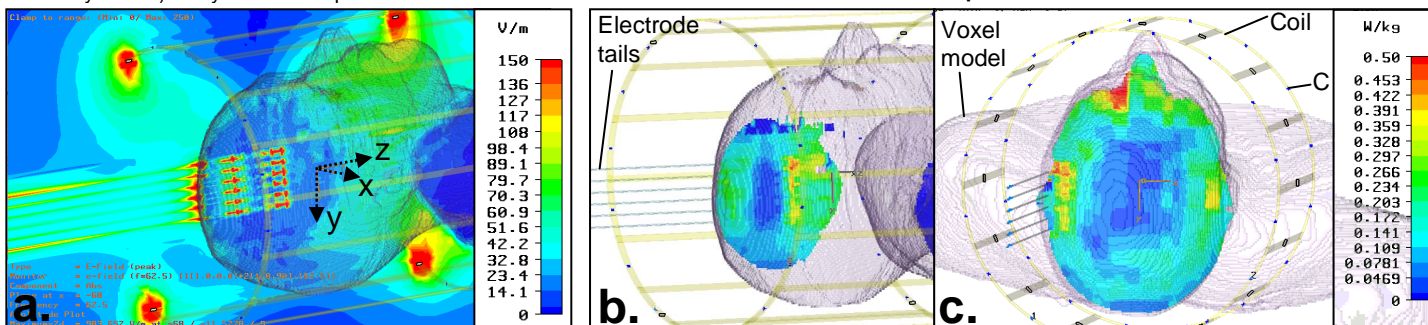


Figure 1 Simulation results: a) The E-field at plane  $x=-68$ mm adjacent to the grid electrodes with peak E-field around the coil, at the grid corners and around the wires before they enter the head, b) SAR-1g, same plane as in 'a' ( $x=-68$ mm) peaking at the anterior-distal contact, c) SAR-1g, at  $z=8$ mm perpendicular to distal grid contacts with a peak near the electrodes but maximum in the sinus area.

**Discussion** The E-field was strongly coupled to the implant and was focused around the distal electrode contacts causing increased local values. However, while the SAR was increased in tissue surrounding the implant the maximum local SAR value was in the same area as for the un-implanted case, even when averaged over 1g of tissue. These results suggest that despite the large increases in local E-field, the relatively small volume over which this increase takes place results in modest local SAR increase averaged over 1g of tissue (the lower mass limit specified in the regulations). The mass over which very high E-fields can be tolerated without leading to highly localised damage is unclear and is likely to be dependant on other factors such as perfusion within that area. These preliminary results were generated using complex models, thus making accuracy difficult to determine. However, in vitro experimentation has shown highly localised heating consistent with the results herein<sup>5</sup>. Further work is needed to validate and extend these results including normalising the results to produce a particular  $B_1$  within the centre of the head which is what an MRI scanner would do in practice (potentially altering coil input power).

**References**

1. Dempsey MF, Condon B. *Thermal injuries associated with MRI*. Clin Radiol. 2001 Jun;56(6):457-65.
2. Hand JW et al. *Prediction of Specific Absorption Rate in Mother and Fetus Associated With MRI Examinations During Pregnancy*. Mag. Reson. Med. 2006, 55:883–893.
3. Weiland TA. *discretization method for the solution of Maxwell's equations for six-component fields*. Electronics Commun (AEU" ) 1977; 31:116–120.
4. Li Y et al. *Numerically-simulated induced electric field and current density within a human model located close to a z-gradient coil*, JMRI 2007, 26:1286-1295.
5. Carmichael DW, et al, *Safety of Localising Intracranial EEG Electrodes Using MRI*, Proc. Int'l. Soc. Mag. Reson. Med. 15 (2007); 1073.